

CONTINUOUS PHASE MODULATION WITH 1-BIT QUANTIZATION USING ADAPTIVE OVERSAMPLING

Rodrigo R. M. de Alencar and Lukas T. N. Landau

Centre for Telecommunications Studies
Pontifical Catholic University of Rio de Janeiro, Rio de Janeiro, Brazil 22453-900
Email: 455.rodrigo.alencar@gmail.com; lukas.landau@cetuc.puc-rio.br

ABSTRACT

Continuous phase modulation (CPM) with 1-bit quantization at the receiver is promising in terms of energy and spectral efficiency. This study proposes a mean square error (MSE) based strategy for selecting the sampling time instances of an oversampled and 1-bit quantized CPM signal. The adaptive sampling scheme is especially suitable for signals with smooth phase transitions such as given by CPM signals based on the raised cosine frequency pulse. Numerical results show that receive processing with the proposed sampling strategy outperforms the conventional receive method based on uniform sampling, while corresponding to a lower computational complexity.

Index Terms— 1-bit quantization, oversampling, continuous phase modulation, adaptive sampling.

1. INTRODUCTION

Continuous phase modulation (CPM) yields spectral efficiency, smooth phase transitions and a constant envelope [1, 2], which allows for the use of energy efficient power amplifiers with low dynamic range. At the receiver side, the energy consumption of the analog-to-digital converter (ADC) scales exponentially with the resolution in amplitude [3]. Hence, in this study a low resolution ADC is considered, where the ADC provides only sign information about the received signal. In order to compensate for the loss in terms of the achievable rate, an adaptive oversampling with respect to the signal bandwidth is considered. In this context, it is shown that uniform oversampling yields a significant gain in terms of achievable rate for the noiseless [4] and for the noisy channel [5]. More recently, high-rate quantization studied in [6] is associated with an adaptive sampling analysis explored in [7], which formulates optimal high-resolution sampling of one-dimensional signals, based on an MSE criterion. Moreover, non-uniform sampling with 1-bit ADCs in large scale MIMO systems is studied in [8]. CPM signals with channels with 1-bit quantization and oversampling has been considered before in [9], where the achievable rate is studied and maximized via optimization of sequences. Later, more practical approaches were proposed in [10], where the intermediate frequency and the waveform is considered in a geometrical analysis of the phase transitions. Moreover, in [11] it is presented how to exploit the channel with 1-bit quantization and oversampling by using iterative detection with sophisticated channel coding for CPM signals.

In this study, an MSE-based nonuniform sampling approach is applied to CPM systems with 1-bit quantization and oversampling at the receiver. As the information is implicitly conveyed in phase transitions of CPM signals, resolution in time explored with adaptive sampling is more promising than resolution of amplitude.

Numerical results confirm that the proposed adaptive sampling is beneficial in terms of achievable rate and bit error rate (BER) in comparison to the state-of-the-art methods [9, 10] using uniform sampling. At the same time the receive processing with the proposed method correspond to lower or equivalent computational complexity.

The rest of the paper is organized as follows: Section 2 defines the system model, whereas Section 3 describes the adaptive sampling process. Section 4 discusses numerical results, while Section 5 gives the conclusions.

Sequences of scalars and vectors are denoted by $x^n = [x_1, \dots, x_n]^T$ and $\mathbf{y}^n = [\mathbf{y}_1^T, \dots, \mathbf{y}_n^T]^T$, respectively. A segment of a sequence is described by $x_{k-L}^k = [x_{k-L}, \dots, x_k]^T$.

2. SYSTEM MODEL

The considered system model is illustrated in Fig. 1, which is based on the discrete time system model proposed in [9] for CPM systems with 1-bit quantization and oversampling at the receiver. A decimation block is replaced by a sample selection strategy with the aim to represent the considered nonuniform sampling, covered in Section 3. In the following, the individual building blocks are detailed.

2.1. CPM Signal Decomposition

The information conveying phase term of the constant envelope CPM signal [1] reads

$$\phi(t) = 2\pi h \sum_{k=0}^{\infty} \alpha_k f(t - kT_s) + \varphi_0, \quad (1)$$

where T_s denotes the symbol duration, $h = K_{\text{cpm}}/P_{\text{cpm}}$ is the modulation index, $f(\cdot)$ is the phase response, φ_0 is a phase-offset and α_k represents the k^{th} transmit symbol. For an even modulation order M_{cpm} , such transmit symbols are taken from an alphabet described by $\alpha_k \in \{\pm 1, \pm 3, \dots, \pm(M_{\text{cpm}} - 1)\}$. In order to obtain a finite number of phase states K_{cpm} and P_{cpm} must be relative prime positive integers. The phase response function $f(\cdot)$ shapes the sequence of CPM symbols to the continuous phase signal with smooth transitions. The phase response is characterized by

$$f(\tau) = \begin{cases} 0, & \text{if } \tau \leq 0, \\ \frac{1}{2}, & \text{if } \tau > L_{\text{cpm}}T_s, \end{cases}$$

where L_{cpm} is the depth of the memory in terms of transmit symbols. As it is depicted in Fig. 2, the phase response corresponds to the integration over the frequency pulse $g_f(\cdot)$. In general, the corresponding phase trellis of (1) is time variant, which means that

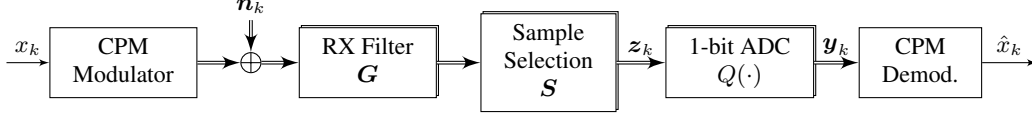


Fig. 1: Discrete time description of the CPM system with 1-bit quantization and oversampling at the receiver

the possible phase states are time-dependent. In order to avoid the time-dependency, a time invariant trellis is constructed by tilting the phase according to the decomposition approach in [12]. The tilt corresponds to a frequency offset applied to the CPM signal, i.e., the phase term becomes $\psi(t) = \phi(t) + 2\pi\Delta f t$, where $\Delta f = h(M_{\text{cpm}} - 1)/2T_s$. By considering the tilted trellis, it is convenient to use a different symbol notation $x_k = (\alpha_k + M_{\text{cpm}} - 1)/2$, which corresponds to the symbol alphabet $\mathcal{X} = \{0, 1, \dots, M_{\text{cpm}} - 1\}$. The tilted CPM phase $\psi(t)$ within one symbol interval with duration T_s , letting $t = \tau + kT_s$, can be fully described by the state definition $\tilde{s}_k = [\beta_{k-L_{\text{cpm}}}, x_{k-L_{\text{cpm}}+1}^k]$ in terms of

$$\begin{aligned} \psi(\tau + kT_s) &= \frac{2\pi}{P_{\text{cpm}}} \beta_{k-L_{\text{cpm}}} \\ &+ 2\pi h \sum_{l=0}^{L_{\text{cpm}}-1} (2x_{k-l} - M_{\text{cpm}} + 1) f(\tau + lT_s) \\ &+ \pi h (M_{\text{cpm}} - 1) \left(\frac{\tau}{T_s} + L_{\text{cpm}} - 1 \right) + \varphi_0, \end{aligned} \quad (2)$$

where the absolute phase state $\beta_{k-L_{\text{cpm}}}$ can be reduced to

$$\beta_{k-L_{\text{cpm}}} = \left(K_{\text{cpm}} \sum_{l=0}^{k-L_{\text{cpm}}} x_l \right) \bmod P_{\text{cpm}},$$

which is related to the 2π -wrapped accumulated phase contributions of the input symbols that are prior to the CPM memory.

The considered discrete time description of the system model implies that the CPM phase is represented in a vector notation. The corresponding tilted CPM phase $\psi(\tau + kT_s)$ for one symbol interval, i.e., $0 < \tau \leq T_s$, is then discretized into MD samples, which composes the vector denoted by $\boldsymbol{\psi}_k(\tilde{s}_k) = [\psi(\frac{\tau}{MD}(kMD + 1)), \psi(\frac{\tau}{MD}(kMD + 2)), \dots, \psi(T_s(k+1))]^T$, where M is the oversampling factor, and D is a higher resolution multiplier. The tilt of the phase can be established in the actual communication system by receiving at an intermediate frequency (IF), which motivates the definition of $\psi_{\text{IF}}(t) = \psi(t) + 2\pi\frac{n_{\text{IF}}}{T_s}t$. With $n_{\text{IF}}P_{\text{cpm}}$ as an integer value, different low-IF frequencies can be used by choosing $n_{\text{IF}} > 0$, which is promising because the appearance of zero-crossings can be adjusted, as proposed in [10]. Hence, such intermediate frequency is

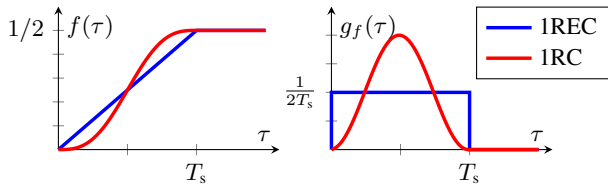


Fig. 2: Frequency pulse shapes (right) and their phase responses (left)

expressed with

$$\left(\Delta f + \frac{n_{\text{IF}}}{T_s} \right) = \frac{h(M_{\text{cpm}} - 1)}{2T_s} + \frac{n_{\text{IF}}}{T_s}. \quad (3)$$

The CPM modulator illustrated in the discrete system model in Fig. 1, takes the input sequence x^n and generates the transmit signal $\sqrt{\frac{E_s}{T_s}} e^{j\psi_k(\tilde{s}_k)}$, where E_s is the symbol energy, i.e., it already takes into account the frequency offset.

2.2. Receive filtering and quantization

The receive filter $g(t)$ has an impulse response of length T_g . In the discrete model for expressing a subsequence of $(\eta + 1)$ oversampling output symbols it is represented in a matrix form with \mathbf{G} , as a $MD(\eta + 1) \times MD(L_g + \eta + 1)$ Toeplitz matrix, whose first row is $[\mathbf{g}^T, \mathbf{0}_{MD(\eta+1)}^T]$, where $\mathbf{g}^T = [g(L_g T_s), g(\frac{T_s}{MD}(L_g MD - 1)), \dots, g(\frac{T_s}{MD})]$. A higher sampling grid in the waveform signal, in the noise generation and in the filtering is adopted to adequately model the aliasing effect. This receive filtering increases the memory of the system by L_g symbols, where $(L_g - 1)T_s < T_g \leq L_g T_s$.

In the discrete system model, the adaptive sampling play its part by selecting M_{eff} samples per symbol from the filtered samples, where M_{eff} is an effective oversampling factor. Such operation is achieved by multiplication with the sample selection matrix \mathbf{S} , which has dimension $M_{\text{eff}}(\eta + 1) \times MD(\eta + 1)$ and is described by

$$S_{i,j} = \begin{cases} 1 & \text{for } j = (\nu_i - 1)D + 1, \\ 0 & \text{otherwise,} \end{cases} \quad (4)$$

where the vector $[\nu_1, \dots, \nu_{M_{\text{eff}}(\eta+1)}]^T$ is chosen such that its entries specify the indexes of the samples that will compose the resulting vector $\mathbf{z}_{k-\eta}^k$, which is 1-bit quantized to the vector $\mathbf{y}_{k-\eta}^k$. These operations can be represented by the following equations

$$\mathbf{y}_{k-\eta}^k = Q(\mathbf{z}_{k-\eta}^k) = Q\left(\mathbf{S} \mathbf{G} \left[\sqrt{\frac{E_s}{T_s}} e^{j\psi_{k-\eta-L_g}} + \mathbf{n}_{k-\eta-L_g}^k \right]\right), \quad (5)$$

where the quantization operator $Q(\cdot)$ is applied element-wise. The quantization of \mathbf{z}_k is described by $y_{k,m} = \text{sgn}(\text{Re}\{z_{k,m}\}) + j \text{sgn}(\text{Im}\{z_{k,m}\})$, where m denotes the oversampling index which runs from 1 to M . The vector $\mathbf{n}_{k-\eta-L_g}^k$ contains complex zero-mean white Gaussian noise samples with variance $\sigma_n^2 = N_0$.

3. ADAPTIVE SAMPLING

This section presents a criterion to describe the sample selection strategy, i.e., the matrix \mathbf{S} , and illustrates the concept for a specific frequency pulse.

3.1. MSE Criterion for Sample Selection

Similarly to [7], this study adopts a MSE criterion to assist the decision for sampling times, which are chosen based on the quantization error averaged over all possible phase transitions. This MSE analysis is done along one symbol duration in a noise free scenario. Let $\Psi_k(\tau)$ the tilted phase description in (2), $0 \leq \tau < T_s$, for a given state \tilde{s}_k , but with the extra frequency offset expressed in (3), i.e., $\Psi_k(\tau) = \psi(\tau + kT_s) + 2\pi n_{\text{IF}}(\tau + kT_s)/T_s$. With the titled CPM symbol described by $\sqrt{E_s/T_s}e^{j\Psi_k(\tau)}$, an MSE concept as function of τ is described by

$$\text{MSE}(\tau) = \frac{1}{n_{st}} \sum_{\tilde{s}_k} \frac{E_s}{T_s} \left| e^{j\Psi_k(\tau)} - \frac{1}{\sqrt{2}} Q \left(e^{j\Psi_k(\tau)} \right) \right|^2, \quad (6)$$

where n_{st} is the number of all possible states \tilde{s}_k and $\frac{1}{\sqrt{2}}Q(\cdot)$ is the normalized 1-bit quantization operator applied continuously over the symbol period.

The Fig. 3 represents some phase transitions of CPM signals with $M_{\text{cpm}} = 8$, $h = 1/M_{\text{cpm}}$, $\phi_0 = \pi/M_{\text{cpm}}$, raised cosine as the frequency pulse (IRC), oversampling factor of $M = 11$, tilted with the frequency offset in (3) with $n_{\text{IF}} = 0.25$. Such scheme is used to illustrate (6) with Fig. 5, where it is possible to realize the best sampling time instances with the minimum values of the graph.

3.2. Case Study on Raised Cosine Frequency Pulse

As proof of concept, this work uses the IRC frequency pulse, vide Fig. 2, as case study for two reasons. First, the use of smooth phase transition reduces the out-of-band radiation, which is a desirable feature for the real-world systems. Second, the existence of near-zero derivative regions of the phase response at the beginning and by the end of the phase transition, promotes a predictable linear behavior for the tilted phase trellis, for which, it is possible to take advantage of such behavior by forcing zero-crossings when the low-IF variable n_{IF} is increased. With this in mind, the estimation of an optimal oversampling factor M and distance between the sampling time instances $d_s T_s/M$, can be done by rewriting (3) as

$$2\pi \left(\frac{h(M_{\text{cpm}} - 1)}{2T_s} + \frac{n_{\text{IF}}}{T_s} \right) = \frac{\Delta\psi}{\Delta\tau} = \frac{2\pi/M_{\text{cpm}}}{d_s T_s/M},$$

which leads to

$$M_{\text{cpm}} (h(M_{\text{cpm}} - 1)/2 + n_{\text{IF}}) = M/d_s. \quad (7)$$

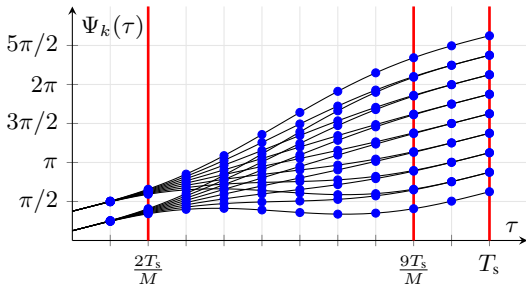


Fig. 3: IRC Tilted phase transitions with, $M_{\text{cpm}} = 8$, $h = 1/M_{\text{cpm}}$, $\phi_0 = \pi/M_{\text{cpm}}$, $n_{\text{IF}} = 0.25$, $M = 11$

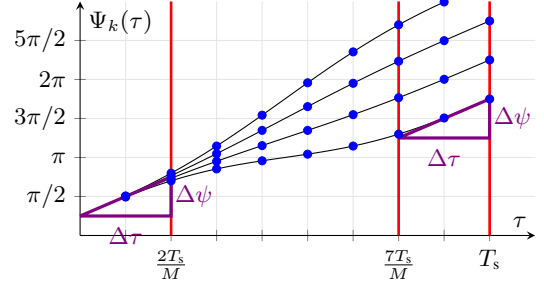


Fig. 4: IRC Tilted phase transitions with $M_{\text{cpm}} = 4$, $h = 1/M_{\text{cpm}}$, $n_{\text{IF}} = 0.75$, $M = 9$

The Fig. 4 illustrates an example for (7), with $M_{\text{cpm}} = 4$, $h = 1/M_{\text{cpm}}$ and $n_{\text{IF}} = 0.75$ the ratio M/d_s becomes $9/2$, which indicates that $M = 9$ is an optimal oversampling factor and the sampling instances at $2T_s/11$, $7T_s/11$ and T_s correspond to the samples with least quantization error. This idea can be reproduced with the case of Fig. 3, where $M/d_s = 11/2$, and verified with the MSE profile in Fig. 5. Note that in Fig. 3 the samples at $9T_s/M$ resolve all the uncertainties brought by the coarse quantization with the sample at T_s , i.e., it would be possible to reach the $\log_2(M_{\text{cpm}}) = 3$ bits per channel use with an effective oversampling factor $M_{\text{eff}} = 2$, using an adaptive nonuniform sampling.

3.3. Receiver Complexity

The adaptive sampling permits the reduction of the number of analyzed samples from M to M_{eff} , which brings less complexity to CPM receivers, that are often carried out with Viterbi or BCJR algorithm. Both algorithms have complexity proportional to the number of all possible state transitions $P_{\text{cpm}} M_{\text{cpm}}^L$ times the number of all possible observed complex vectors 4^M , which is a consequence of the oversampling (factor M) and 1-bit quantization (4-level phase).

The soft detection realized via a BCJR algorithm [13] based on an auxiliary channel law $W(\mathbf{y}_k | \mathbf{y}_{k-1}, x^n) = P(\mathbf{y}_k | \mathbf{y}_{k-N}^{k-1}, x^n)$, that considers the dependency on N previous channel realizations, relies on an extended state representation

$$s_k = \begin{cases} [\beta_{k-L+1}, x_{k-L+2}^k], & \text{if } L > 1, \\ [\beta_k], & \text{if } L = 1. \end{cases} \quad (8)$$

where $L = L_{\text{cpm}} + L_g + N$ is the overall memory. As input for the algorithm, the channel output probabilities $P(\mathbf{y}_{k-N} | s_k, s_{k-1})$

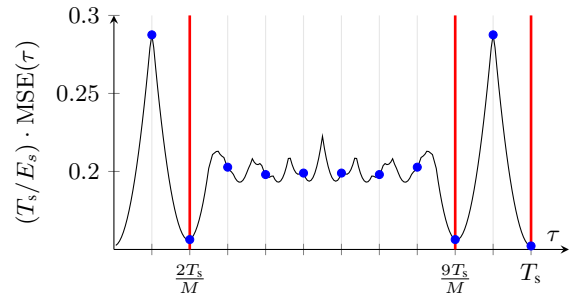


Fig. 5: MSE profile for the scenario in Fig. 3

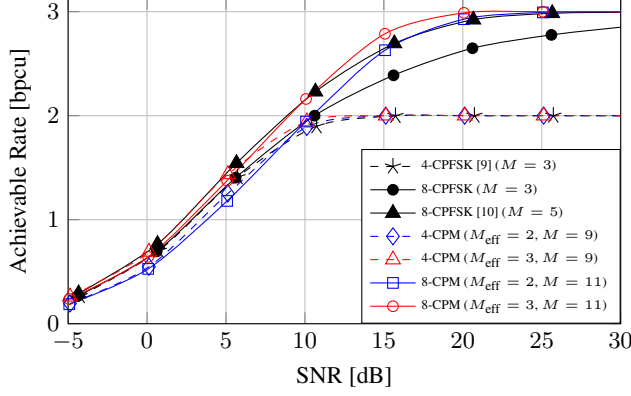


Fig. 6: Achievable Rate of the considered CPM waveforms

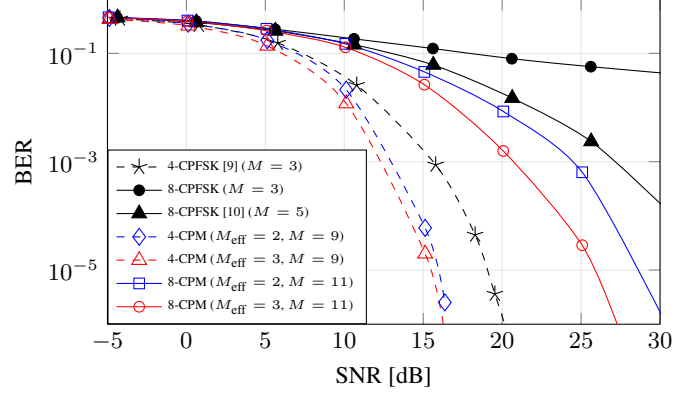


Fig. 7: BER performance of the considered CPM waveforms

involve a multivariate Gaussian integration in terms of

$$P\left(\mathbf{y}_{k-N}^k | s_k, s_{k-1}\right) = \int_{\mathbf{z}_{k-N}^k \in \mathcal{V}_{k-N}^k} p\left(\mathbf{z}_{k-N}^k | s_k, s_{k-1}\right) d\mathbf{z}_{k-N}^k, \quad (9)$$

where \mathbf{z}_{k-N}^k is a complex Gaussian random vector that describes the input of the 1-bit ADC, with a mean vector defined by $\mathbf{m}_x = \mathbf{S} \mathbf{G} \left[\sqrt{E_s T_s} e^{j\psi_{k-N-L_g}} \right]$, and covariance matrix $\mathbf{K}_z = \sigma_n^2 \mathbf{S} \mathbf{G} \mathbf{G}^H \mathbf{S}^T$, with \mathbf{S} and \mathbf{G} as introduced before with $\eta = N$. The integration interval is expressed in terms of the quantization region \mathcal{V}_{k-N}^k that belongs to the channel output symbol \mathbf{y}_{k-N}^k . After rewriting (9) as a real valued multivariate Gaussian integration, shown in [9], the algorithm in [14] can be applied. However, as detailed in [10], the number of evaluations of (9) required for the model, is proportional to $4^M M_{\text{cpm}}^L$, which is computationally expensive when the oversampling factor M , the modulation order M_{cpm} and the overall channel memory L are high valued, a point to be improved by using adaptive sampling.

4. NUMERICAL RESULTS

With the purpose to preserve the transmit waveform and its crossings on the 1-bit quantization levels, a suboptimal short bandpass receive filter is considered as follows

$$g(t) = \sqrt{\frac{1}{T_g}} \text{rect}\left(\frac{t - T_g/2}{T_g}\right) \cdot e^{j2\pi\Delta f(t - T_g/2)}, \quad (10)$$

with $T_g = 0.5T_s$, which is similar to the integrate and dump receiver considered in [15], but with its frequency response centered in low-IF. For the considered CPM waveforms the following simulation parameters are chosen:

- **4-CPFSK [9]** : 1REC, $M_{\text{cpm}} = 4$, $M = 3$, $n_{\text{IF}} = 0$;
- **8-CPFSK [10]** : 1REC, $M_{\text{cpm}} = 8$, $M = 3$ and 5 , $n_{\text{IF}} = 0.25$;
- **4-CPM ($M_{\text{eff}} = 2$)** : 1RC, $\nu^{M_{\text{eff}}} = [7, 9]^T$, $M_{\text{cpm}} = 4$, $M = 9$, $n_{\text{IF}} = 0.75$ (Fig. 4);
- **4-CPM ($M_{\text{eff}} = 3$)** : 1RC, $\nu^{M_{\text{eff}}} = [2, 7, 9]^T$, $M_{\text{cpm}} = 4$, $M = 9$, $n_{\text{IF}} = 0.75$ (Fig. 4);
- **8-CPM ($M_{\text{eff}} = 2$)** : 1RC, $\nu^{M_{\text{eff}}} = [9, 11]^T$, $M_{\text{cpm}} = 8$, $M = 11$, $n_{\text{IF}} = 0.25$ (Fig. 3);

- **8-CPM ($M_{\text{eff}} = 3$)** : 1RC, $\nu^{M_{\text{eff}}} = [2, 9, 11]^T$, $M_{\text{cpm}} = 8$, $M = 11$, $n_{\text{IF}} = 0.25$ (Fig. 3);

with $L_{\text{cpm}} = 1$, $h = 1/M_{\text{cpm}}$, $\phi_0 = \pi/M_{\text{cpm}}$, $N = 0$. 4-CPFSK [9] and 8-CPFSK [10] serve as reference waveforms that use uniform sampling and 1REC frequency pulse described in Fig. 2. The adjustable power containment bandwidth $B_{90\%}$ is considered, where we refer to 90% power containment as default. With this, the adopted SNR definition is

$$\text{SNR} = \frac{\lim_{T \rightarrow \infty} \frac{1}{T} \int_T |x(t)|^2 dt}{N_0 B_{90\%}} = \frac{E_s}{N_0} (T_s B_{90\%})^{-1}, \quad (11)$$

where $x(t) = \sqrt{E_s/T_s} e^{j\psi(t)}$ is the complex low-IF representation of the signal and N_0 is the noise power density.

4.1. Achievable Rate

The method to compute a lower-bound on the achievable rate is explored in [9, 16], where an auxiliary channel law is considered. Fig. 6 illustrates how the increase of the effective oversampling factor can benefit the information rate results. The results confirm that based on the adaptive sampling scheme the full rate of 8-CPM signals can be achieved with 2-fold oversampling ($M_{\text{eff}} = 2$) at high SNR.

4.2. Bit Error Rate

All BER results, from Fig. 7, has been computed using the BCJR algorithm that implies the auxiliary channel law. In comparison to uniform sampling, a significant benefit can be observed when using the adaptive sampling with the same or less number of samples.

5. CONCLUSIONS

This study proposes a novel adaptive oversampling technique for CPM signals with 1-bit quantization. The proposed method optimizes the sampling time instances based on an MSE criterion. Numerical results show that the corresponding receiver with nonuniform sampling provides a better BER performance when compared to receivers with a higher complexity that use uniform sampling.

ACKNOWLEDGMENT

This work has been supported by the ELIOT ANR18-CE40-0030 and FAPESP 2018/12579-7 project.

6. REFERENCES

- [1] J. Anderson, T. Aulin, and C. E. Sundberg, *Digital Phase Modulation*, Plenum Press, New York, 1986.
- [2] C. E. Sundberg, "Continuous phase modulation," *IEEE Commun. Mag.*, vol. 24, no. 4, pp. 25–38, April 1986.
- [3] R.H. Walden, "Analog-to-digital converter survey and analysis," *IEEE J. Sel. Areas Commun.*, vol. 17, no. 4, pp. 539–550, Apr. 1999.
- [4] S. Shamai (Shitz), "Information rates by oversampling the sign of a bandlimited process," *IEEE Trans. Inf. Theory*, vol. 40, no. 4, pp. 1230–1236, July 1994.
- [5] L. Landau, M. Dörpinghaus, and G. P. Fettweis, "1-bit quantization and oversampling at the receiver: Communication over bandlimited channels with noise," *IEEE Commun. Lett.*, vol. 21, no. 5, pp. 1007–1010, May 2017.
- [6] R. M. Gray and D. L. Neuhoff, "Quantization," *IEEE Trans. Inf. Theory*, vol. 44, no. 6, pp. 2325–2383, Oct 1998.
- [7] Y. Dar and A. M. Bruckstein, "On high-resolution adaptive sampling of deterministic signals," *Journal of Mathematical Imaging and Vision*, vol. 61, no. 7, pp. 944–966, 2019.
- [8] Z. Shao, L. T. N. Landau, and R. C. de Lamare, "Dynamic oversampling for 1-bit ADCs in large-scale multiple-antenna systems," *IEEE Trans. Commun.*, 2021.
- [9] L. T. N. Landau, M. Dörpinghaus, R. C. de Lamare, and G. P. Fettweis, "Achievable rate with 1-bit quantization and oversampling using continuous phase modulation-based sequences," *IEEE Trans. Wireless Commun.*, vol. 17, no. 10, pp. 7080–7095, Oct 2018.
- [10] S. Bender, M. Dörpinghaus, and G. P. Fettweis, "The potential of continuous phase modulation for oversampled 1-bit quantized channels," in *Proc. of the IEEE Int. Workshop on Signal Processing Advances in Wireless Communications*, Cannes, France, July 2019.
- [11] R. R. M. de Alencar, L. T. N. Landau, and R. C. de Lamare, "Continuous phase modulation with 1-bit quantization and oversampling using soft detection and iterative decoding," *EURASIP J. Wireless Commun. Netw.*, vol. 2020, no. 237, 2020.
- [12] B. E. Rimoldi, "A decomposition approach to CPM," *IEEE Trans. Inf. Theory*, vol. 34, no. 2, pp. 260–270, Mar. 1988.
- [13] L. Bahl, J. Cocke, F. Jelinek, and J. Raviv, "Optimal decoding of linear codes for minimizing symbol error rate (corresp.)," *IEEE Trans. Inf. Theory*, vol. 20, no. 2, pp. 284–287, Mar. 1974.
- [14] A. Genz, "Numerical computation of multivariate normal probabilities," *Journal of Computational and Graphical Statistics*, pp. 141–149, 1992.
- [15] M. H. M. Costa, "A practical demodulator for continuous phase modulation," in *Proc. IEEE Int. Symp. Inform. Theory (ISIT)*, Trondheim, Norway, Jun 1994, p. 88.
- [16] L. T. N. Landau, M. Dörpinghaus, and G. P. Fettweis, "1-bit quantization and oversampling at the receiver: Sequence-based communication," *EURASIP J. Wireless Commun. Netw.*, vol. 2018, no. 83, 2018.